Bioorganic & Medicinal Chemistry 18 (2010) 5685–5696

Contents lists available at ScienceDirect

Bioorganic & Medicinal Chemistry

journal homepage: www.elsevier.com/locate/bmc

Synthesis and biological evaluation of novel pyrazole compounds

Amal M. Youssef [a,b], Edward G. Neeland [a], Erika B. Villanueva [c], M. Sydney White [c], Ibrahim M. El-Ashmawy [d], Brian Patrick [e], Andis Klegeris [c,*], Alaa S. Abd-El-Aziz [a,*]

[a] Department of Chemistry, University of British Columbia Okanagan, Kelowna, BC, Canada
[b] Department of Pharmaceutical Chemistry, Faculty of Pharmacy, University of Alexandria, Alexandria, Egypt
[c] Department of Biology, University of British Columbia Okanagan, Kelowna, BC, Canada
[d] Department of Pharmacology, Faculty of Veterinary Medicine, University of Alexandria, Alexandria, Egypt
[e] X-ray Facility, University of British Columbia Vancouver, BC, Canada

ARTICLE INFO

Article history:
Received 28 April 2010
Revised 4 June 2010
Accepted 5 June 2010
Available online 12 June 2010

Keywords:
Pyrazoles
Anti-inflammatory drugs
Neuroprotection

ABSTRACT

A novel dipyrazole ethandiamide compound and acid chloride of pyrazolo[3,4-*d*]pyrimidine 4(5H)-one were prepared and reacted with a number of nucleophiles. The resultant novel compounds were tested in several in vitro and in vivo assays. Three compounds inhibited the secretion of neurotoxins by human THP-1 monocytic cells at concentrations that were not toxic to these cells. They also partially inhibited both cyclooxygenase-1 and -2 isoforms. In animal studies, two compounds were notable for their anti-inflammatory activity that was comparable to that of the clinically available cyclooxygenase-2 inhibitor celecoxib. Modeling studies by using the molecular operating environment module showed comparable docking scores for the two enantiomers docked in the active site of cyclooxygenase-2.

1. Introduction

Pyrazole and pyrazolopyrimidine compounds have been reported as therapeutic agents for a diverse number of applications. Pyrazole derivatives have been proposed as potential treatments for neurodegenerative disorders like Alzheimer's disease, Parkinson's disease, and bovine spongiform encephalopathy.[1] Pyrazoles are also active antitumour,[2] anticonvulsant,[3] and antimicrobial agents.[4] They are used for pain relief[5] and have shown success in the inhibition of the human immunodeficiency virus.[6] Pyrazole derivatives are insecticides[7] and are used in dyeing.[8]

Pyrazolopyrimidine compounds are equally widespread in diversity. They may act as Trk and c-Src inhibitors,[9] C–C chemokine receptor type 1 (CCR1) and purine antagonists,[10] HIV reverse transcriptase inhibitors[11] as well as showing activity as antitumour/antileukemia,[12] and herbicidal/fungicidal[13] agents. Like the pyrazoles, pyrazolopyrimidines are used in the dyeing industry.[14] Pyrazolopyrimidines are also used to treat insomnia.[15]

We were most interested in the anti-inflammatory properties of pyrazoles and pyrazolo[3,4-*d*]pyrimidines as potential inhibitors of cyclooxygenase (COX)[16] and p38α[17] isoenzymes. Non-steroidal anti-inflammatory drugs (NSAIDs), which are known to inhibit COX enzymes, are currently used as important therapeutic agents for the treatment of pain and inflammation. Celecoxib (aka: Celebrex®, Celebra®, Niflam®, and Onsenal®), a COX-2-selective NSAID is a pyrazole derivative. Celecoxib has relatively few gastrointestinal (GI) side effects but its long-term use is associated with cardiovascular injury, which limits its clinical applications.[18] Therefore, there is a need for the development of novel drugs with better safety profiles that could be used long-term to relieve chronic inflammatory conditions. Our starting point was synthesizing new derivatives of pyrazoles and investigating how structural changes affected their anti-inflammatory and neuroprotective properties.

2. Results and discussion

2.1. Chemistry

Popular methods for making a pyrazole ring system react a hydrazine moiety with a molecule possessing β-electrophilic centers. These centers are represented by α,β-unsaturated carbonyl,[19] α,β-unsaturated nitrile,[12c] β-ketocarbonyl,[3,5a] or β-nitrilocarbonyl functionalities[2a,9a,10b,20] (Scheme 1).

Other approaches to pyrazoles react a substituted hydrazine with an α-chlorocarbonyl group.[21] Once formed, the pyrazole rings can be further elaborated to pyrazolopyrimidines using formamide or urea,[10b,22] chromenones,[23] or base catalyzed cyclization.[12d,24,25]

We followed a modified method of Cheng[10b] whereby phenylhydrazine and ethoxymethylenemalonitrile reacted to produce

* Corresponding authors. Tel.: +1 250 807 9557; fax: +1 250 807 8005 (A.K.); tel.: +1 250 807 9139; fax: +1 250 807 9005 (A.S.A.).
E-mail addresses: andis.klegeris@ubc.ca (A. Klegeris), alaa.abd-el-aziz@ubc.ca (A.S. Abd-El-Aziz).

0968-0896/$ - see front matter © 2010 Elsevier Ltd. All rights reserved.
doi:10.1016/j.bmc.2010.06.018

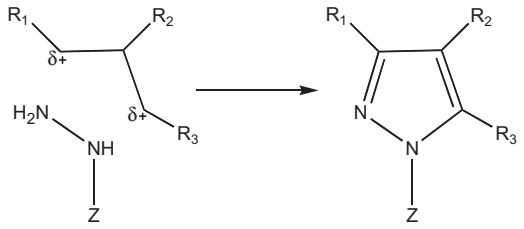

Scheme 1. Formation of the pyrazole ring.

2-amino-3-nitrilo-1-phenylpyrazole **1**. Reaction of **1** with oxalyl chloride followed by nucleophilic attack was expected to yield substituted pyrazolo[3,4-*d*]pyrimidines **2** (Scheme 2).

In our hands, this reaction gave an 85% yield of a crystalline parent compound, which cleanly reacted with a variety of amine nucleophiles. However, the spectral analysis showed that the parent compound had nine unique carbon atoms, possessed a nitrile functionality and an independent phenyl substituted pyrazole ring. This suggested that the pyrazole amine **1** had undergone a bimolecular addition with the oxalyl chloride to yield the dipyrazole ethandiamide compound **3** (Scheme 3).

Heterocyclic ethandiamide derivatives like this are infrequently reported but not unknown.[1a,1b,4d,26] Suitable crystals of **3** were analyzed by X-ray crystallography and the Oakridge Thermal Ellipsoid Plot (ORTEP) confirmed the dipyrazole ethandiamide structure (Fig. 1).

With the structure of the parent compound **3** in hand, we turned our attention to the products which had incorporated the amine nucleophiles. The amine adducts did not exist as tautomeric Schiff bases[27] of compound **3**. Two dimensional NMR data from correlation spectroscopy (COSY-45) and heteronuclear multiple quantum coherence (HMQC) identified two imine (NH) hydrogens of which one NH showed *J*-coupling with the substituent R group and the other NH was uncoupled. This pattern is inconsistent with the Schiff base structure. A nuclear Overhauser enhancement (NOE) was also observed between the NH adjacent to the pyrazole ring and the ortho phenyl hydrogen. Furthermore, heteronuclear multiple bond coherence (HMBC) correlations were observed between one NH and carbonyl carbon atom as well as between the methine (CH) of the amine substituent and the other carbonyl carbon atom (Fig. 2).

These data, taken together, were more suggestive of a monopyrazolo diamide **4** resulting from a pyrazole displacement by the amine nucleophile (Scheme 4).

To avoid going through the intermediate compound **3**, the structure of **4a** was confirmed via an independent synthesis in this order: oxalyl chloride, phenethylamine, and pyrazole **1**. Curiously, no evidence of both pyrazole rings being displaced in these reactions was observed. Despite reacting **3** with 10 equiv of phenethylamine and substantially increasing the reaction time, compound **4a** was still isolated resulting from the loss of only one pyrazole ring. Further attempts to displace the second pyrazole ring in **4a** with excess NH_4OH only produced starting material. The reluctance of the second pyrazole ring to leave may be attributed to its carbonyl group being inductively stabilized by the newly introduced and more electron-donating amino substituent.

The formation and reactivity of the dipyrazole ethandiamide **3** suggested a revised synthetic route to make the originally desired pyrazolo[3,4-*d*]pyrimidine **2**. Very slow addition of pyrazole **1** to an excess of oxalyl chloride produced the acid chloride of pyrazolo[3,4-*d*]pyrimidine which was immediately reacted with methanol to yield the methyl ester **2** (Fig. 3).

This series of unique compounds, dipyrazole ethandiamide **3**, pyrazole ethandiamides **4a–f**, and the methyl pyrazolo[3,4-*d*]pyrimidine ester **2**, were subsequently tested for potential anti-inflammatory and neuroprotective properties.

2.2. In vitro assays

The above compounds were initially tested in several in vitro assays to assess their cytotoxic, anti-inflammatory, and anti-neurotoxic properties. Figures 4–7 show data obtained by using the lead compound **3**, while Table 1 summarizes data obtained in the same assays by using all six of the newly synthesized compounds as well as a standard anti-inflammatory drug celecoxib.

2.2.1. Monocytic cell viability and chemokine secretion

First, human monocytic THP-1 cells were pre-incubated with experimental drugs or the vehicle solution dimethyl sulfoxide (DMSO) for 15 min before their stimulation with a combination of lipopolysaccharide (LPS) and interferon (IFN)-γ. Viability of THP-1 cells and secretion of a pro-inflammatory chemokine monocyte chemoattractant protein-1 (MCP-1) by these cells were assessed 24 h later. Figure 4 shows that at 500 μM, compound **3** caused a significant reduction in the percentage of viable THP-1 cells (Fig. 4A) and increased lactate dehydrogenase (LDH) concentration in the supernatants, which indicates increased cellular lysis (Fig. 4B). Only the highest concentration of compound **3** studied (500 μM) caused a reduction in MCP-1 levels after the 24 h incubation period (Fig. 5), which was most likely caused by the direct toxicity to THP-1 cells. Table 1 illustrates that the inhibitory effects of compound **2** and celecoxib on MCP-1 secretion were similarly due to their direct toxicity. Meanwhile the IC_{50} for compound **4d** on MCP-1 secretion (Table 1) was lower than the EC_{50} for its toxic effect, which may indicate a selective anti-inflammatory activity of this compound.

2.2.2. Anti-neurotoxic effects

Figure 6 illustrates the anti-neurotoxic effect of compound **3**, which was assessed by measuring the viability of human neuronal SH-SY5Y cells after their exposure to THP-1 cell supernatants for 72 h. In previous studies,[28] supernatants from unstimulated THP-1 cells did not cause a reduction of SH-SY5Y cell viability and LDH levels were comparable to those obtained after incubation of SH-SY5Y cells in growth medium only (data not shown). Transfer of

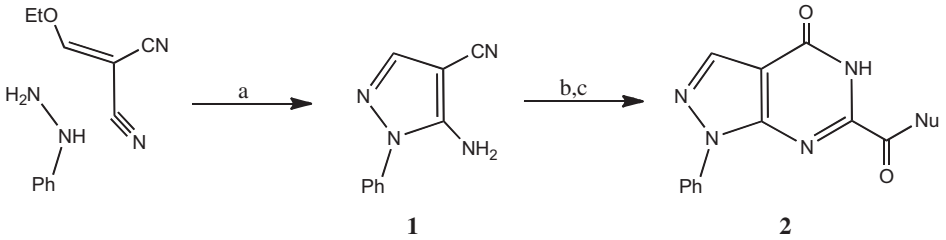

Scheme 2. Reagents and condition: (a) EtOH, reflux; (b) $(COCl)_2$; (c) Nu^-.

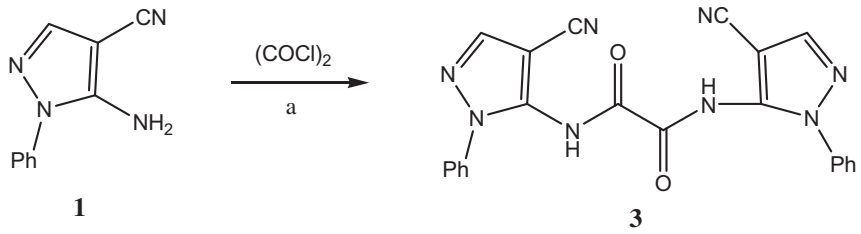

Scheme 3. Formation of the diadduct with oxalyl chloride. Reagent and condition: (a) THF, rt.

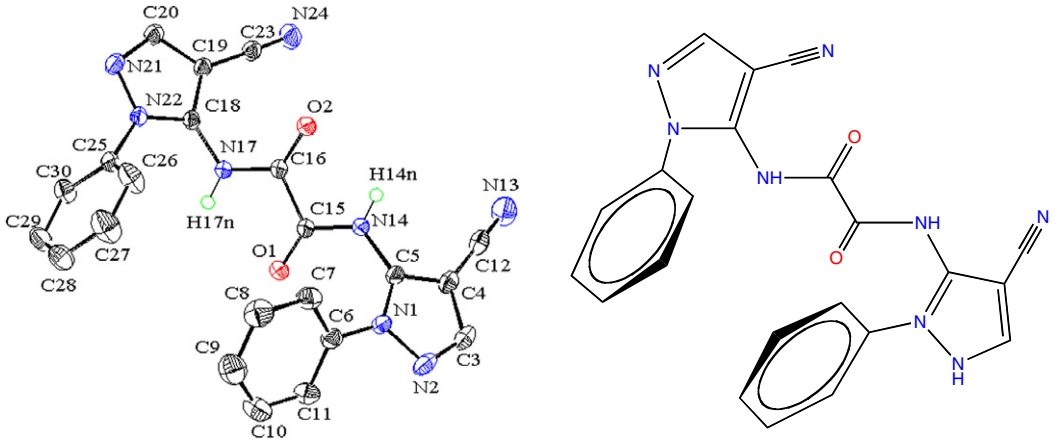

Figure 1. ORTEP plot and structure of **3**; 50% probability thermal ellipsoids; selected bond lengths (Å) and angles (°): C(15)–C(16) 1.5308 (16), C(15)–O(1) 1.2134 (14), C(15)–N(14) 1.3539 (15), C(5)–N(14) 1.3942 (15), C(5)–C(4) 1.3872 (17), C(5)–N(1) 1.3536 (16), C(4)–C(12) 1.4235 (19), C(4)–C(3) 1.4057 (18), C(12)–N(13) 1.1492 (19), C(3)–N(2) 1.3198 (18), N(2)–N(1) 1.3737 (14), N(1)–C(6) 1.4352 (16); N(2)–C(3)–C(4) 112.01 (11), C(5)–C(4)–C(3) 104.45 (11), C(5)–C(4)–C(12) 127.03 (12), C(3)–C(4)–C(12) 128.52 (12), N(1)–C(5)–N(14) 124.85 (11), C(15)–N(14)–C(5) 123.65 (10), N(14)–C(15)–C(16) 111.90 (10), N(13)–C(12)–C(4) 178.54 (14), O(1)–C(15)–N(14) 125.95 (11).

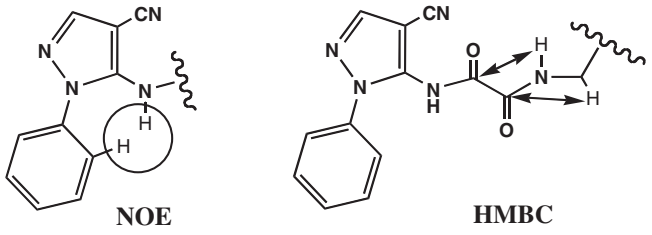

Figure 2. Diagnostic NOE and HMBC correlations in compound **4**.

supernatants from THP-1 cells that had been stimulated with LPS + IFN-γ caused a significant reduction in SH-SY5Y cell viability and increase in LDH content in cell supernatants. Addition of 10–100 μM of compound **3** to THP-1 cells 15 min prior to their stimulation reduced the neurotoxicity of THP-1 cell secretions. At the highest concentration of 500 μM, there was pronounced neuronal death, again, most likely caused by direct toxic effect of compound **3** that was transferred with supernatants to the neuronal cells. We confirmed that compound **3** was directly toxic to the SH-SY5Y cells by applying it at 5–500 μM to SH-SY5Y cultures and measuring cell viability 72 h later. According to the MTT assay, compound **3** caused an 86% and 23% reduction in cell viability at 500 and 100 μM, respectively (data not shown).

With the completion of the pilot study, six of the newly synthesized compounds plus the reference anti-inflammatory drug celecoxib were tested in the assays described above and the results are summarized in Table 1.

Both MTT and LDH assays were performed to assess the cytotoxic and anti-neurotoxic effects of compounds and the corre-

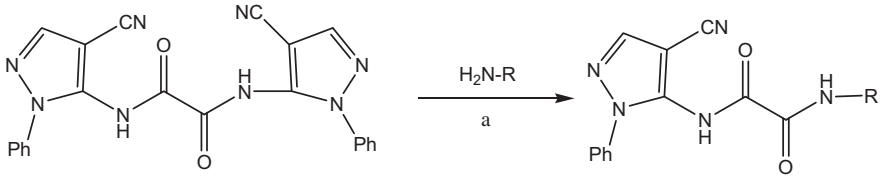

3

4a: R= -CH_2CH_2Ph
4b: R= -$CH_2CH_2CH_2$morpholino
4c: R= -cyclohexyl
4d: R= -(±)-methylbenzyl
4e: R= -(+)-methylbenzyl
4f: R= -(-)-methylbenzyl

Scheme 4. Pyrazole diamide derivatives **4**. Reagent and condition: (a) THF, reflux.

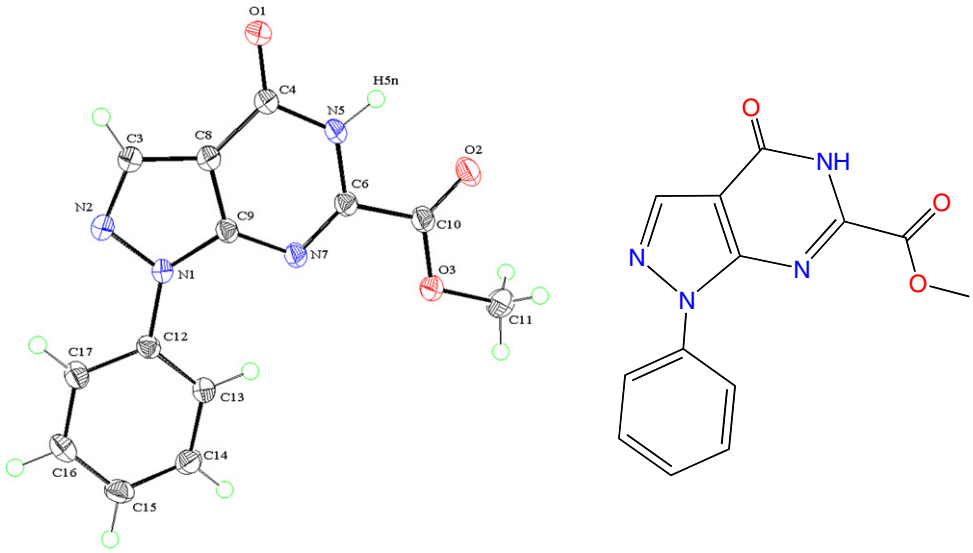

Figure 3. ORTEP plot and structure of **2**; 50% probability thermal ellipsoids; selected bond lengths (Å) and angles (°): N(1)–N(2) 1.3765 (13), N(1)–C(12) 1.4311 (14), N(1)–C(9) 1.3662 (14), N(2)–C(3) 1.3176 (15), C(3)–C(8) 1.4044 (16), C(8)–C(9) 1.3891 (15), C(8)–C(4) 1.4319 (16), C(4)–O(1) 1.2297 (15), C(4)–N(5) 1.3912 (15), N(5)–C(6) 1.3657 (14), C(6)–N(7) 1.3015 (14), C(6)–C(10) 1.45103 (15), N(7)–C(9) 1.3686 (14); N(2)–C(3)–C(8) 110.91 (11), O(1)–C(4)–N(5) 121.82 (11), O(1)–C(4)–C(8) 126.61 (11), N(5)–C(4)–C(8) 111.57 (10), C(9)–C(8)–C(3) 105.66 (10), N(1)–C(9)–N(7) 127.00 (10), N(7)–C(6)–N(5) 126.00 (10), N(5)–C(6)–C(10) 113.48 (10), N(7)–C(9)–C(8) 126.43 (10).

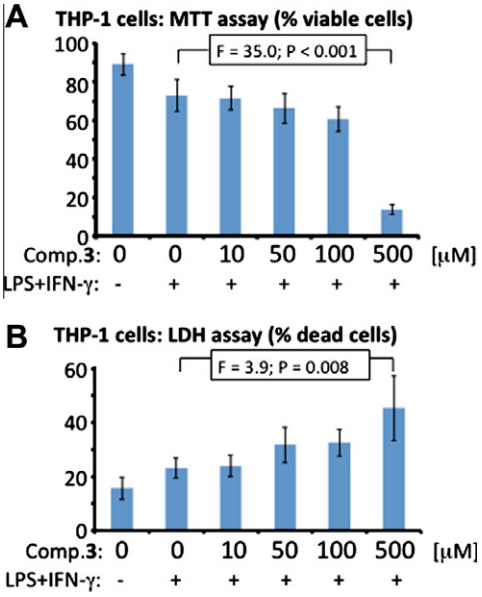

Figure 4. Direct toxicity of compound **3** on stimulated human monocytic THP-1 cells. Cells were seeded into 24-well plates at a concentration of 4.5×10^5 cells per well in 0.9 mL of DMEM-F12 medium containing 5% fetal bovine serum (FBS). They were pretreated with various concentrations (μM) of inhibitors (shown on the abscissa) for 15 min before stimulation with lipopolysaccharide (LPS) (0.5 mg mL^{-1}) and IFN-γ (150 U mL^{-1}). After 24 h incubation, the THP-1 cell viability was assessed by the MTT assay (A) and by measuring the LDH activity in the supernatants (B). Data (means ± SEM) from 11 independent experiments are presented. The concentration-dependent effects of compound **3** were assessed by randomized block design ANOVA; F and P values obtained for each of the drug treatments are presented in the figure.

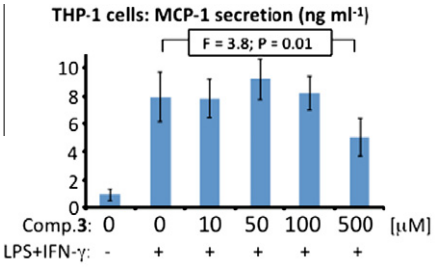

Figure 5. Effect of compound **3** on the secretion of the pro-inflammatory chemokine MCP-1 by human monocytic THP-1 cells. Cells were treated as described in the legend of Figure 4. MCP-1 concentration in cell-free supernatants was measured by enzyme linked immunoabsorbent assay (ELISA). Data (means ± SEM) from eight independent experiments are presented. The concentration-dependent effect of compound **3** was assessed by randomized block design ANOVA.

sponding EC_{50} and IC_{50} values were estimated. The lower concentration value is presented in the table where the values obtained by two assays differed. Two of the compounds (**4b** and **4c**) showed no significant effects in the three assays used. Compound **4a** was highly toxic to THP-1 cells with EC_{50} = 10 μM and therefore it was not tested in other assays. Compounds **2**, **3**, **4d**, and celecoxib, although toxic to THP-1 cells at high concentrations, inhibited monocytic cell neurotoxicity at significantly lower concentrations. The difference between the toxic and anti-neurotoxic effect was lowest for compound **2** (40 μM vs 20 μM); there was a 10-fold difference for compound **3** (100 μM vs 10 μM) and celecoxib (50 μM vs 5 μM); and the highest difference was for compound **4d**, which was toxic to THP-1 cells with an EC_{50} of 500 μM, while its anti-neurotoxic effects had an IC_{50} of 14 μM and 6 μM according to the MTT and LDH assays, respectively. Compounds **2**, **3**, and **4d** were therefore selected for further studies.

2.2.3. COX enzymatic activity

A COX inhibitor screening assay showed that all three compounds partially inhibited both COX isoforms, while celecoxib, as expected, was active mainly against the COX-2 enzyme (Table 2). It is important to note that this assay was used as a general inhibitor screening tool; more accurate measurements, such as O_2 uptake assay, will be needed in order to obtain accurate estimates of IC_{50} for the newly synthesized drugs.[29]

2.2.4. Neuroprotective effects

The direct neuroprotective effects of compounds **2**, **3**, and **4d** were also assessed. Addition of compound **3** directly to SH-SY5Y cells at the time of transfer of supernatants from stimulated

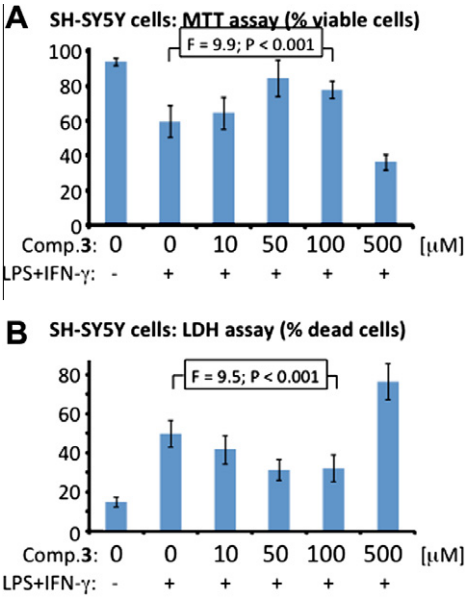

Figure 6. Compound **3** in a concentration-dependent manner inhibits toxicity of THP-1 cell secretions toward SH-SY5Y neuroblastoma cells. THP-1 cells were pretreated with various concentrations (μM) of inhibitors as described in the legend of Figure 4. After 24 h incubation, the cell-free supernatants of THP-1 cells were transferred to the wells containing SH-SY5Y cells. Viability of SH-SY5Y cells was assessed after 72 h by the MTT assay (A) and by measuring the LDH activity in the supernatants (B). Data (means ± SEM) from 11 independent experiments are presented. The concentration-dependent effects of compound **3** were assessed by randomized block design ANOVA.

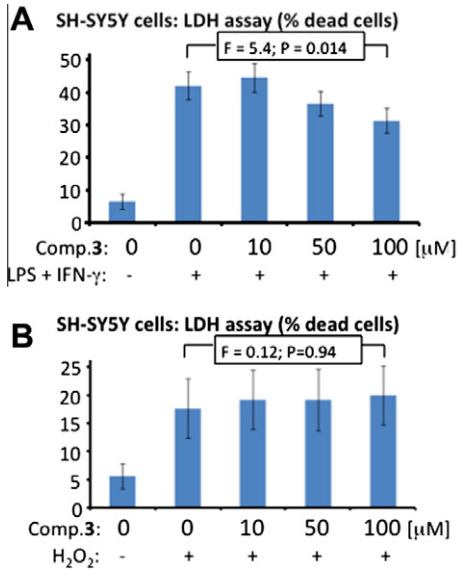

Figure 7. Compound **3** in a concentration-dependent manner protects SH-SY5Y cells from THP-1 cell secretion-induced toxicity, but not from hydrogen peroxide-induced lysis. SH-SY5Y cells were seeded into 24-well plates at a concentration of 2×10^5 cells mL^{-1} in 0.4 mL of DMEM-F12 medium containing 5% FBS. Various concentrations of compound **3** were added at the time of transfer of THP-1 cell supernatants that had been stimulated with LPS + IFN-γ (A) or culture media containing 250 μM H_2O_2. Cell death was assessed by the LDH assay 72 h later. Data (means ± SEM) from five independent experiments are presented. The concentration-dependent effects of compound **3** were assessed by randomized block design ANOVA.

THP-1 cells resulted in a concentration-dependent reduction in neuronal killing according to the LDH assay (Fig. 7A). Compound **3** failed to rescue SH-SY5Y cells killed by hydrogen peroxide (H_2O_2) which is often used to model oxidative stress in cell culture experiments (Fig. 7B).[30] Compounds **2** and **4d** were ineffective as neuroprotective agents when added directly to SH-SY5Y cells independent of the agent used to induce neuronal death (data not shown). In the case of compound **3**, its direct neuroprotective effect on SH-SY5Y cells (Fig. 7A) could also be at least partially responsible for its effect in the anti-neurotoxic assay (Fig. 6B) since some of the compound could have been transferred to SH-SY5Y cultures with the supernatants from stimulated THP-1 cells.

Table 1
Comparative in vitro biological activity of pyrazole derivatives

Compound	Concentration (μM)	THP-1 cytotoxicity EC_{50} (μM)	THP-1 secretion of MCP-1 IC_{50} (μM)	Anti-neurotoxic effect IC_{50} (μM)
2	0.5–500	**40**[a]	**100**	**20**
3	5–500	**100**	**250**	**10**
4a	0.5–500	**10**	Not tested	Not tested
4b	5–500	>500	>500	100
4c	5–500	80	>500	250
4d	1–1000	**500**	**150**	**6**
Celecoxib	5–100	**50**	**70**	**5**

[a] Bold values indicate assays where the concentration-dependent effects of the compounds were statistically significant ($P < 0.05$, randomized block design ANOVA). Cytotoxicity, inhibition of MCP-1 secretion and anti-neurotoxic activity (inhibition of THP-1 toxicity towards SH-SY5Y cells) were assessed as described for compound **3** in Figures 4–6, respectively.

Table 2
Inhibition of cyclooxygenase (COX-1 and COX-2) enzymatic activity

Compound	Concentration (number of experiments)	COX-1 activity (% inhibition)	COX-2 activity (% inhibition)
2	100 μM (4)	16.4 ± 4.1	14.2 ± 5.0
3	100 μM (4)	11.2 ± 3.4	14.0 ± 3.3
4d	100 μM (4)	24.5 ± 5.2	33.8 ± 19.2
Celecoxib	10 μM (3)	0.3 ± 2.5	30.8 ± 5.9

2.2.5. Anti-neurotoxic activity of 4d enantiomers

The separate enantiomers of **4d** ((+) = **4e** and (−) = **4f**) were each compared with the racemic mixture. Data presented in Figure 8 are comparable to those in Figure 6, except for the fact that THP-1 cells were incubated in the presence of various compounds and stimulus for 48 h instead of 24 h. The longer 48 h incubation time was chosen to achieve more severe neurotoxicity. Longer stimulation period of THP-1 cells indeed resulted in a higher percentage of SH-SY5Y cell death (cf. Figs. 8 and 6). Also, the anti-neurotoxic effect of compound **4d** was somewhat reduced with the IC_{50} values increasing to 14 μM according to the MTT assay (Fig. 8A) and 40 μM according to the LDH measurements (Fig. 8B). Both enantiomers, **4e** and **4f**, showed activity similar to the racemic mixture **4d**. These results further narrowed the list of candidates for in vivo experiments to compounds **3**, **4d**, and its enantiomers **4e** and **4f**.

We previously reported that NSAIDs (which act by inhibiting COX) diminished THP-1 cell-induced toxicity towards SH-SY5Y cells in vitro.[28] Here we demonstrate that compounds **2**, **3**, and **4d–f** were reducing neuronal cell killing by THP-1 cells. All five of these compounds, similarly to the previously studied NSAIDs, were able to reduce the toxic secretions thus demonstrating anti-neurotoxic activity on stimulated THP-1 cells. Since these compounds partially inhibit both COX isoforms (Table 2), it is likely that their in vitro anti-neurotoxic activity is mediated through the inhibition of prostaglandin production by THP-1 cells.[28b] Compound **3** had an additional benefit by protecting SH-SY5Y cells

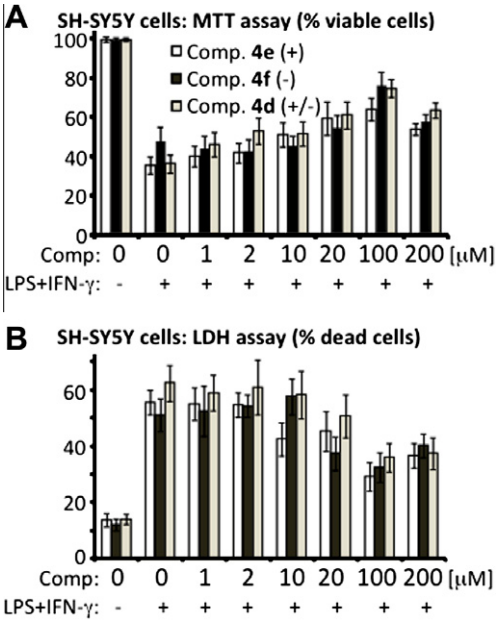

Figure 8. Compounds **4**–**f** show similar anti-neurotoxic effect on THP-1 cell-mediated killing of SH-SY5Y cells. Experiments were performed as described in the legend of Figure 6 except that THP-1 cells were incubated in the presence of stimuli and compounds for 48 h instead of 24 h. Data (means ± SEM) from 11 independent experiments are presented. All compounds displayed statistically significant concentration-dependent effects ($P < 0.05$) according to the randomized block design ANOVA.

from THP-1 cell toxic secretions (Fig. 7A); the biochemical mechanisms responsible for this effect remain to be elucidated.

2.3. In vivo assays

The anti-inflammatory activity of selected analogs **3**, **4d**, **4e** and **4f** were evaluated by two screening protocols, namely, the formalin-induced paw edema and turpentine oil-induced granuloma pouch bioassays. Celecoxib (20 mg/kg) was used as a reference standard anti-inflammatory agent. The paw edema was employed as a model for acute and sub-acute inflammation, while the turpentine oil-induced granuloma pouch assay was utilized as another model for sub-acute inflammatory condition. The data obtained are presented in Tables 3–5.

2.3.1. Formalin-induced paw edema bioassay

In this acute inflammatory model each test compound was dosed orally (po) at 20 mg/kg body weight 1 h prior to induction of inflammation by formalin injection. Celecoxib was utilized as a reference anti-inflammatory drug at a dose of 20 mg/kg, po. The anti-inflammatory activity was then calculated at 1, 2, 3, and 4 h after induction. The data are presented in Table 3 as the mean paw volume (mL) and the percentage anti-inflammatory activity.

All of the test compounds, including celecoxib, significantly reduced paw edema volume 1, 2, 3, and 4 h after induction. However, a comparison of the anti-inflammatory activity of the test compounds, relative to the control, indicated distinctive pharmacokinetic profiles. Thus, after 1 h, compounds **4d** (50%) and **4e** (56%) showed a potent and more rapid onset of action than celecoxib (38%). After 2 h, only compound **3** was equally as effective as celecoxib in inhibiting the paw edema. After a 3 h time interval compounds **3**, **4d**, and **4e** displayed good anti-inflammatory activity (38–50%), but none superior to the reference drug. However, after 4 h, the anti-inflammatory activity of compounds **3** (58%), **4d** (50%), and **4e** (50%) were equal to or higher than that of celecoxib (47%).

Table 4
Anti-inflammatory activity of compounds in formalin-induced rat paw edema bioassay (sub-acute inflammatory model)

Compound[a]	Volume of edema[b] (mL)		
	0	1st day	8th day
Control	0.29 ± 0.01	0.75 ± 0.01	0.83 ± 0.01
3	0.31 ± 0.02	0.57 ± 0.01* (43)	0.61 ± 0.01* (44)
4d	0.30 ± 0.01	0.58 ± 0.01* (39)	0.63 ± 0.01* (38)
4e	0.31 ± 0.01	0.59 ± 0.01* (39)[c]	0.67 ± 0.02* (33)
4f	0.28 ± 0.02	0.55 ± 0.01* (41)	0.63 ± 0.01* (35)
Celecoxib	0.30 ± 0.01	0.59 ± 0.02* (37)	0.67 ± 0.02* (41)

* Significantly different compared to respective control values, $P < 0.05$.
[a] Dose levels of 20 mg/kg (po) were used for all test compounds including celecoxib.
[b] Values are expressed as means ± SEM ($N = 5$ rats per experimental group).
[c] Values in parentheses (percentage anti-inflammatory activity).

Table 5
Anti-inflammatory activity of compounds in the turpentine oil-induced granuloma pouch model

Compound[a]	Volume of exudates[b] (mL)	Percentage of inhibition
Control	2.05 ± 0.03	—
3	0.99 ± 0.03*	48
4d	1.00 ± 0.06*	51
4e	1.24 ± 0.06*	39
4f	1.03 ± 0.04*	49
Celecoxib	1.10 ± 0.05*	46

* Significantly different compared to respective control values, $P < 0.05$.
[a] Dose levels of 20 mg/kg (po) were used for all test compounds including celecoxib.
[b] Values are expressed as means ± SEM ($N = 5$ rats per experimental group).

Table 3
Anti-inflammatory activity of compounds in formalin-induced rat paw edema bioassay (acute inflammatory model)

Compound[a]	Volume of edema[b] (mL)				
	0	1 h	2 h	3 h	4 h
Control	0.29 ± 0.01	0.45 ± 0.01	0.51 ± 0.01	0.61 ± 0.01	0.67 ± 0.01
3	0.31 ± 0.02	0.40 ± 0.04* (44)[c]	0.44 ± 0.01* (41)	0.47 ± 0.01* (50)	0.47 ± 0.01* (58)
4d	0.30 ± 0.01	0.38 ± 0.01* (50)	0.46 ± 0.01* (27)	0.47 ± 0.02* (46)	0.49 ± 0.01* (50)
4e	0.31 ± 0.01	0.38 ± 0.01* (56)	0.45 ± 0.01* (36)	0.49 ± 0.01* (44)	0.50 ± 0.01* (50)
4f	0.28 ± 0.02	0.38 ± 0.03* (37)	0.43 ± 0.02* (32)	0.48 ± 0.02* (38)	0.51 ± 0.02* (39)
Celecoxib	0.30 ± 0.01	0.40 ± 0.02* (38)	0.43 ± 0.02* (41)	0.46 ± 0.01* (56)	0.50 ± 0.01* (47)

* Significantly different compared to respective control values, $P < 0.05$.
[a] Dose levels of 20 mg/kg (po) were used for all test compounds including celecoxib.
[b] Values are expressed as means ± SEM ($N = 5$ rats per experimental group).
[c] Values in parentheses represent percentage anti-inflammatory activity.

Table 6
The anti-inflammatory activity (ED_{50}), ulcerogenic effects, and acute LD_{50} of test compounds

Test compound	ED_{50} (mg/kg)	% Ulceration	ALD_{50} (mg/kg)
Indomethacin	—	100	—
3	17.50	0.0	>300
4d	19.64	10.0	>300
4e	18.95	0.0	>300
4f	22.41	0.0	>300
Celecoxib	15.65	0.0	—

2.3.2. Formalin-induced paw edema bioassay (sub-acute inflammatory model)

In this sub-acute inflammatory model, inflammation was induced by formalin injection on the first and third days, and test compounds were administered orally (at 20 mg/kg daily) for 7 days. Again, celecoxib was used as a reference anti-inflammatory agent in this assay. The anti-inflammatory activity was calculated at the 1st and 8th day after induction and the data presented in Table 4 as the mean paw volume and the percentage anti-inflammatory activity relative to a control.

The obtained data revealed that, according to the measurements performed on both the 1st and 8th day, all tested compounds displayed significant anti-inflammatory activity. Percent inhibition on the 1st day was the highest for compound **3** (43%), which was greater than celecoxib (37%). At the 8th day, compound **3** was found to have an anti-inflammatory activity higher than the reference drug with a percentage inhibition of 44% while compound **4d** was nearly effective (38%) as celecoxib (41%).

2.3.3. Turpentine oil-induced granuloma pouch bioassay

In this sub-acute inflammatory model, each test compound was administered orally (20 mg/kg) 1 h prior to turpentine oil injection and administration was continued for 7 days. At the 8th day, the volume of exudates (mL) was measured and the percentage of granuloma inhibition was calculated. Celecoxib (20 mg/kg) was used as a reference drug. Table 5 illustrates that all of the studied compounds significantly reduced the exudate volume when compared to the control group of animals. Compounds **4d**, **4f**, and **3** appeared to be more potent than celecoxib (46%) with percentages of granuloma inhibition of 51%, 49%, and 48%, respectively.

The in vivo experiments (Tables 3–5) demonstrated anti-inflammatory activity of compounds **3** and **4d** in formalin paw edema model of acute inflammation, as well as in the formalin paw edema and turpentine oil-induced granuloma pouch assays (sub-acute inflammatory models). Therefore these compounds might be effective in managing acute inflammation, as well as in controlling chronic inflammatory conditions.

2.3.4. Effective dose 50 (ED_{50}) in formalin-induced paw edema bioassay

The tested compounds were further evaluated for their ED_{50} in male rats 3 h after formalin injection. The results indicated that compounds **3**, **4d**, and **4e** have ED_{50} similar to celecoxib suggesting that they were nearly equipotent to the reference drug.

2.3.5. Ulcerogenic activity

The tested compounds that exhibited variable anti-inflammatory profiles were further evaluated for their ulcerogenic potential in rats. Gross observation of the isolated rat stomachs showed a normal stomach texture for all of the tested compounds with no observable hyperemia. This indicated a superior GI safety profile (0–10% ulceration) in the population of the fasted rats. It is noteworthy that, indomethacin—the reference standard anti-inflammatory drug—caused 100% ulceration under the same experimental conditions (Table 6).

2.3.6. Acute toxicity

All of the selected compounds were further evaluated for their approximate acute lethal dose (ALD_{50}) in male rats. All of the

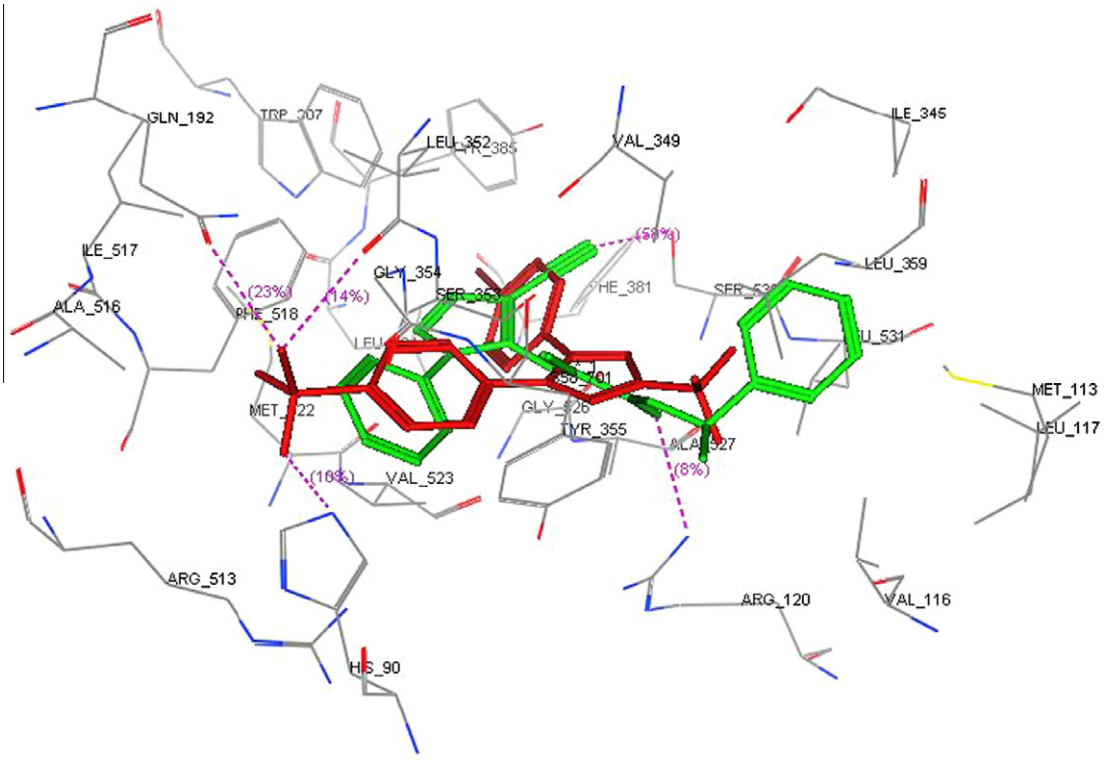

Figure 9. COX-2 superimposition of the co-crystallized celecoxib derivative SC-558 (colored red) and the docked compound **4e** (colored green). Pink dashed lines depict hydrogen bond interactions. Viewed using MOE module.

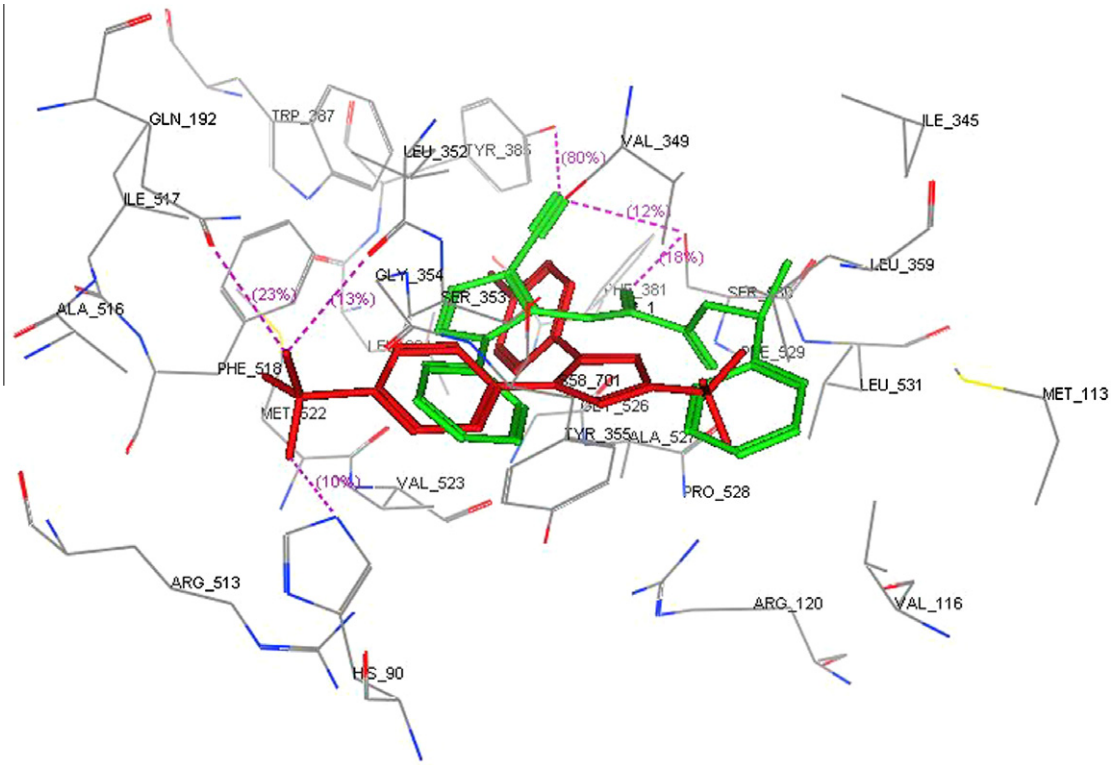

Figure 10. COX-2 superimposition of the co-crystallized celecoxib derivative SC-558 (colored red) and the docked compound **4f** (colored green). Pink dashed lines depict hydrogen bond interactions. Viewed using MOE module.

tested compounds proved to be non-toxic and well-tolerated by the experimental animals. The compounds showed a high safety margin when screened at graded doses (10–300 mg/kg, po), where their ALD_{50} values were found to be >300 mg/kg (Table 6).

3. Docking study

The inhibition of the COX-2 enzyme by compound **4d** (Table 2) encouraged us to investigate the structural basis underlying the docking of both enantiomers **4e** and **4f**. The docking study was carried out using the enzyme parameters obtained from the crystallographic structure of the complex between COX-2 with the co-crystallized celecoxib derivative SC-558 (PDB ID: 1CX2).[31] The docking simulation for the ligands was carried out using molecular operating environment (MOE) software supplied by the Chemical Computing Group, Inc., Montréal Canada.[32]

In the SC-558 molecule, hydrogen bonding is shown between the oxygen atom and the imidazole NH His90, and also between the sulfonamide NH_2 group of SC-558, the carbonyl oxygen of Gln192 and carbonyl oxygen of Leu35. Whereas in compound **4e**, hydrogen bonding is observed between the nitrogen of the cyano group and hydroxyl group of Ser530 as well as between the carbonyl oxygen of compound **4e** with the NH of Arg120 (Fig. 9).

Figure 10 shows COX-2 superimposition of SC-558 and the docked (−)-enantiomer **4f**. In this case, hydrogen bonding is observed between the cyano group nitrogen and both the hydroxyl groups of Tyr385 and Ser530. Hydrogen bonding is also seen between the carbonyl oxygen of compound **4f** and the hydroxyl group of Ser530.

In Figures 9 and 10, the methyl benzyl group of enantiomers **4e** and **4f** adopt the same position as the trifluoromethyl group of SC-558 and is bound in a hydrophobic cavity formed by Met113, Val116, Val349, and Leu359. In addition, the *N*-phenyl ring of compounds **4e** and **4f** adopts the same position as the *p*-sulfamoylphenyl moiety of SC-558 and is surrounded by hydrophobic residues Tyr355, Ph518, and Val523. The docking study shows that the enantiomeric compounds **4e** and **4f** have a binding pattern in the COX-2 site which is close to the pattern observed in the crystal structure of the SC-558 complex with comparable docking scores. This may account for the in vitro COX-2 inhibition recorded for the racemic mixture (Table 2). These observations may also explain the very similar anti-neurotoxic activity of the two enantiomers (Fig. 8).

4. Conclusion

A novel dipyrazole ethandiamide lead compound **3** has been synthesized and derivatized through the nucleophilic displacement of only one pyrazole group. The resultant novel ethandiamide compounds have been investigated for possible anti-inflammatory and neuroprotective properties using human cell lines as surrogates of glial and neuronal cells. In vitro cell culture techniques and enzymatic assays were utilized to screen the compounds for their ability to affect a number of biological properties including: (1) cell viability; (2) secretion of a pro-inflammatory chemokine; (3) the COX enzymatic activity and (4) monocytic cell-induced killing of neuronal cells. The synthesized compounds were also evaluated for their in vivo anti-inflammatory activity using two different screening protocols, namely, formalin-induced paw edema and the turpentine oil-induced granuloma pouch bioassays.

Among the tested analogs, compounds **2**, **3**, and **4d** showed in vitro anti-neurotoxic and neuroprotective activity at concentrations below their toxic range and partially inhibited both COX-1 and COX-2 enzymes. It should be noted that both enantiomers **4e** and **4f** showed in vitro activity as anti-neurotoxic agents very similar to the racemic mixture **4d**. Comparable docking scores with the COX-2 enzyme active site also suggested that **4e** and **4f** may

possess similar anti-inflammatory properties in line with the in vitro results. Compounds **3** and **4d** were notable for their more potent and faster onset of action than the clinically available COX-2 inhibitor celecoxib in both the acute inflammatory and sub-acute inflammatory models. This suggests that they might be effective in managing acute inflammation, as well as in controlling chronic inflammatory conditions. Additionally, all of the selected compounds revealed excellent GI safety profile and were well-tolerated by experimental animals with a high safety margin (ALD_{50} >300 mg/kg). Finally, compound **4d** was identified as a novel neuroprotective and anti-inflammatory agent within this study. Compounds **3** and **4d** were the most efficacious derivatives and represented sterically smaller and more lipophilic molecules in comparison to the other derivatives. These attributes may have facilitated their passage through cell membranes and accounted for their activity. Future work will attempt to confirm this hypothesis through a systematic and rigorous battery of derivatizations of various ethandiamide parent compounds. The pyrazole ethandiamide compounds represent a fruitful matrix for the future development of a new class of neuroprotective and anti-inflammatory agents.

5. Experimental

5.1. Chemistry

Unless otherwise specified, all reagents were used as supplied by either the Sigma–Aldrich-Fluka (St. Louis, MO, USA) or Fisher Scientific (Ottawa, ON, Canada) chemical companies. Reaction solvents were dried by storage over 3 Å molecular sieves. Melting points were determined in open glass capillaries on a Stuart melting point apparatus and are uncorrected. IR spectra in cm^{-1} were recorded on a FTIR Nicolet IR 200 spectrophotometer. ^1H NMR and ^{13}C NMR spectra were run on an AS 400 MHz NMR Oxford Spectrophotometer, using tetramethylsilane (TMS) as the internal standard and DMSO-d_6 as the solvent. Chemical shifts were recorded as δ (ppm). Mass spectrometry data was collected by time of flight mass spectrometry (Micromass LCT Premier TM series (ToF) MS; Waters Inc.). The system was set up to acquire in positive electrospray ionization (ESI+) in W mode. The following source parameters were used for instrumental analysis: capillary voltage (2900 V), sample cone voltage (30 V), desolvation temperature (350 °C), source temperature (120 °C), gas flow through the cone (20 mL/min), and desolvation gas flow (750 mL/min). The optical parameters of the instrument were as follows: aperture 1 voltage (15 V), ion energy (35 V), aperture 2 voltage (4.0 V), hexapole voltage (5.0 V), attenuated Z focus voltage (250 V), ToF flight tube voltage (7200 V), reflection voltage (1800 V), pusher (940 V), puller voltage (820 V), and MCP detector voltage (2050 V). Purity of all samples was determined using elemental analyses with an EA 1108 elemental analyzer. Reactions were monitored by TLC analysis using Merck Silica Gel 60 F-254 thin layer plates. Flash chromatography was carried out on silica gel (230–400 mesh). All compounds showed purities equal to or greater than 95% as determined by elemental analysis.

5.1.1. Methyl 4,5-dihydro-4-oxo-1-phenyl-1*H*-pyrazolo[3,4-*d*]pyrimidine-6-carboxylate (2)

To a stirred solution of oxalyl chloride (1.27 g, 0.01 mol) in THF (5 mL), a solution of 5-amino-1-phenyl-1*H*-pyrazole-4-carbonitrile **1** (0.92 g, 0.005 mol) in THF (5 mL) was added dropwise over a period of 2 h. The reaction mixture was further stirred for 24 h at rt. The solvent was evaporated under reduced pressure, and the formed product was filtered, dried and refluxed in excess methanol for 5 min. The beige crystals were collected by suction filtration in an 84% yield; mp 160–162 °C; IR (cm^{-1}): 1735 (CO), 1692 (CO amide); ^1H NMR (δ ppm): 12.85 (s, 1H, NH, D_2O exchangeable), 8.42 (s, 1H, pyrazole-C_5–H), 8.02–7.42 (m, 5H, aromatic-H), 3.93 (s, 1H, CH_3); ^{13}C NMR (δ ppm): 160.1, 157.1, 150.8, 146.3, 137.9, 136.3, 129.4, 127.6, 122.1, 108.5, 53.7. Calculated for ($C_{13}H_{11}N_4O_3$ = M+1) 271.0831, found 271.0811.

5.1.2. N^1,N^2-Bis(4-cyano-1-phenyl-1*H*-pyrazol-5-yl)oxalamide (3)

To a stirred solution of 5-amino-1-phenyl-1*H*-pyrazole-4-carbonitrile **1** (1.84 g, 0.01 mol) in tetrahydrofuran (THF) (10 mL) was added oxalyl chloride (1.27 g, 0.01 mol) dropwise over a period of 30 min. The reaction mixture was stirred for further 24 h at room temperature (rt). The solvent was evaporated under reduced pressure, diethyl ether is then added and the product was filtered and recrystallized from methanol (yield 85%); mp 262–264 °C; IR (cm^{-1}): 3218 (NH), 2237 (CN), 1689 (CO amide); ^1H NMR (δ ppm): 11.78 (s, 1H, NH, D_2O exchangeable), 8.35 (s, 1H, pyrazole-C_5–H), 7.53–7.46 (m, 5H, aromatic-H); ^{13}C NMR (δ ppm): 157.8, 142.7, 139.3, 137.3, 129.5, 129.1, 123.8, 112.4, 90.5. Calculated for ($C_{22}H_{15}N_8O_2$ = M+1) 423.1318, found 423.1357.

5.1.3. 2-Oxo-2-substituted-*N*-[4-cyano-1-phenyl-1*H*-pyrazol-5-yl] acetamides (4)

A mixture of oxalamide derivative **4** (0.42 g, 0.001 mol) and the appropriate amine (0.004 mol) in dry THF (10 mL) was heated under reflux for 2 h. The solvent was evaporated under reduced pressure, diethyl ether added and the formed product was filtered, washed with diethyl ether, dried and crystallized from chloroform–hexane.

5.1.3.1. 2-Oxo-2-phenethylamino-*N*-[4-cyano-1-phenyl-1*H*-pyrazol-5-yl] acetamide (4a). Yield 80%; mp 168–170 °C; IR (cm^{-1}): 3229 (NH), 2232 (CN); ^1H NMR (δ ppm): 9.13 (s, 1H, NH, D_2O exchangeable), 8.33 (s, 1H, pyrazole-C_5–H), 7.54–7.15 (m, 10H, aromatic-H), 3.36 (q, 2H, J = 8 HZ, CH_2), 2.78 (t, 2H, J = 8 Hz, CH_2); ^{13}C NMR (δ ppm): 159.7, 157.9, 142.5, 138.9, 137.2, 129.4, 128.9, 128.6, 128.3, 126.2, 123.8, 112.4, 90.4, 40.6, 34.3. Calculated for ($C_{20}H_{18}N_5O_2$ = M+1) 360.1461, found 360.1453.

5.1.3.2. 2-Morpholinopropyl 2-oxo-*N*-[4-cyano-1-phenyl-1*H*-pyrazol-5-yl] acetamide (4b). Yield 82%; mp 138–140 °C; IR (cm^{-1}): 3227 (NH), 2234 (CN); ^1H NMR (δ ppm): 9.72 (s, 1H, NH, D_2O exchangeable), 8.94 (s, 1H, pyrazole-C_5–H), 8.53–8.23 (m, 5H, aromatic-H), 4.07 (t, 2H, J = 6 Hz, CH_2), 3.37 (t, 2H, J = 6 Hz, CH_2), 2.49–2.47 (m, 6H, CH_2); ^{13}C NMR (δ ppm): 159.7, 157.9, 142.1, 138.5, 128.9, 127.5, 123.3, 114.2, 90.4, 66.1, 56.2, 53.3, 40.1, 25.3. Calculated for ($C_{19}H_{23}N_6O_3$ = M+1) 383.1831, found 383.1838.

5.1.3.3. 2-Cyclohexylamino-2-oxo-*N*-[4-cyano-1-phenyl-1*H*-pyrazol-5-yl] acetamide (4c). Yield 82%; 212–213 °C; IR (cm^{-1}): 3229 (NH), 2234 (CN); ^1H NMR (δ ppm): 8.99 (s, 1H, NH, D_2O exchangeable), 8.30 (s, 1H, pyrazole-C_5–H), 7.7–7.3 (m, 5H, aromatic-H), 1.7–1.2 (m, 10H, CH_2); ^{13}C NMR (δ ppm): 159.9, 157.2, 142.5, 137.3, 129.4, 128.9, 123.9, 112.5, 90.2, 48.7, 31.6, 24.7. Calculated for ($C_{18}H_{20}N_5O_2$ = M+1) 338.1617, found 338.1585.

5.1.3.4. *R/S*-(±)-2-Methylbenzylamino 2-oxo-*N*-[4-cyano-1-phenyl-1*H*-pyrazol-5-yl] acetamide (4d). Yield 85%; mp 180–182 °C; IR (cm^{-1}): 3229 (NH), 2220 (CN); ^1H NMR (δ ppm): 8.07 (s, 1H, NH, D_2O exchangeable), 7.70 (s, 1H, pyrazole-C_5–H), 7.7–7.35 (m, 10H, aromatic-H), 4.35 (q, 1H, J = 7.2 Hz, CH), 1.44 (d, 3H, J = 7.2 Hz, CH_3); ^{13}C NMR (δ ppm): 161.9, 148.1, 142.1, 139.6, 138.5, 128.9, 128.7, 128.4, 127.4, 126.7, 123.3, 114.5, 86.2, 50.0, 20.9. Calculated for ($C_{20}H_{18}N_5O_2$ = M+1) 360.1460, found 360.1461.

5.1.3.5. *R*-(+)-2-Methylbenzylamino 2-oxo-*N*-[4-cyano-1-phenyl-1*H*-pyrazol-5-yl] acetamide (4e). Yield 85%; mp 180–182 °C; IR, ^{1}H NMR, ^{13}C NMR same as above. Calculated for ($C_{20}H_{18}N_5O_2$ = M+1) 360.1460, found 360.1457.

5.1.3.6. *S*-(−)-2-Methylbenzylamino 2-oxo-*N*-[4-cyano-1-phenyl-1*H*-pyrazol-5-yl] acetamide (4f). Yield 83%; mp 180–182 °C; IR, ^{1}H NMR, ^{13}C NMR same as above. Calculated for ($C_{20}H_{18}N_5O_2$ = M+1) 360.1460, found 360.1449.

5.2. In vitro assays

5.2.1. In vitro reagents

The following substances used in various assays were obtained from Sigma: hydrogen peroxide, bacterial lipopolysaccharide (LPS, from *Escherichia coli* 055:B5), diaphorase (EC 1.8.1.4, from *Clostridium kluyveri,* 5.8 U mg^{-1} solid), DMSO, *p*-iodonitrotetrazolium violet, NAD$^+$, MTT (3-(4,5-dimethylthiazol-2-yl)-2,5-diphenyl tetrazolium bromide). Human recombinant IFN-γ, MCP-1 and antibodies used in MCP-1 enzyme linked immunoabsorbent assay (ELISA) were purchased from Peprotech (Rocky Hill, NJ, USA).

5.2.2. Cell culture

The human monocytic THP-1 cell line was obtained from the American Type Culture Collection (ATCC, Manassas, VA, USA). The human neuroblastoma SH-SY5Y cell line was a gift from Dr. R. Ross, Fordham University, NY. These cells were grown in Dulbecco's modified Eagle's medium-nutrient mixture F12 ham (DMEM-F12) supplemented with 10% fetal bovine serum (FBS) supplied by Thermo Scientific HyClone (Logan, UT, USA). Both cell lines were used without initial differentiation.

5.2.3. Effects of compounds on THP-1 cells viability and MCP-1 secretion

Human monocytic THP-1 cells were seeded into 24-well plates at a concentration of 5×10^5 cells mL^{-1} in 0.9 mL of DMEM-F12 medium containing 5% FBS. The cells were incubated in the presence or absence of various compounds or their vehicle solution (DMSO) for 15 min prior to the addition of an activating stimulus (0.5 μg mL^{-1} LPS with 150 U mL^{-1} IFN-γ). After 24 h incubation, 100 μL of THP-1 culture media were sampled for lactate dehydrogenase (LDH) to determine percentage of dead cells, while evaluation of surviving cells was performed by the MTT assay. In addition, concentration of MCP-1 (ng mL^{-1}) was measured in 100 μL of cell-free culture medium by ELISA according to the protocol provided by the supplier of the antibodies (Peprotech).

5.2.4. Cytotoxicity of THP-1 cells toward SH-SY5Y neuroblastoma cells

THP-1 cells were seeded into 24-well plates and stimulated in the presence and absence of various compounds as described above. After 24 or 48 h incubation, 0.4 mL of cell-free supernatant was transferred to each well containing SH-SY5Y cells. The cells had been plated 24 h earlier at a concentration of 2×10^5 cells mL^{-1} in 0.4 mL of DMEM-F12 medium containing 5% FBS. After 72 h of incubation, the neuronal culture media were sampled for LDH to determine release from dead cells, while evaluation of surviving cells was performed by the MTT assay.

5.2.5. Neuroprotective effects

SH-SY5Y cells were seeded into 24-well plates at a concentration of 2×10^5 mL^{-1} in 0.4 mL of DMEM-F12 medium containing 5% FBS. After 24 h incubation cell culture medium was replaced by either supernatants form THP-1 cells that had been stimulated for 24 h with LPS + IFN-γ or culture media containing 250 μM H_2O_2. Various concentrations of the compounds were added directly to the SH-SY5Y cells at the time of transfer of media. Cell death was assessed by the LDH assay 72 h later.

5.2.6. Cell viability assays: LDH release

Cell death was evaluated by LDH release. LDH activity in cell culture supernatants was measured by an enzymatic test in which formation of the formazan product of iodonitrotetrazolium dye was followed colorimetrically.[33] Briefly, 100 μL of cell culture supernatants were pipetted into the wells of 96-well plates, followed by addition of 15 μL lactate solution (36 mg mL^{-1}) and 15 μL *p*-iodonitrotetrazolium violet solution (2 mg mL^{-1}). The enzymatic reaction was started by addition of 15 μL of NAD$^+$/diaphorase solution (3 mg mL^{-1} NAD$^+$; 2.3 mg solid mL^{-1} diaphorase). After 15–30 min incubation, the reaction was terminated by addition of 15 μL oxamate (16.6 mg mL^{-1}). Optical densities at 490 nm were measured by a microplate reader, and the amount of LDH which had been released was expressed as a fraction of the value obtained in comparative wells where the remaining cells were totally lysed by 1% Triton X-100.

5.2.7. Cell viability assays: reduction of formazan dye (MTT)

The MTT assay was performed using a previously described method,[34] which is based on the ability of viable, but not dead cells, to convert the tetrazolium salt (MTT) to colored formazan. The viability of SH-SY5Y cells was determined by adding MTT to the SH-SY5Y cell cultures to reach a final concentration of 0.5 mg mL^{-1}. Following a 1 h incubation at 37 °C, the dark crystals formed were dissolved by adding to the wells an equal volume of SDS/DMF extraction buffer (20% sodium dodecyl sulfate, 50% *N*,*N* dimethyl formamide, pH 4.7). Subsequently, plates were placed overnight at 37 °C; optical densities at 570 nm were then measured by transferring 100 μL aliquots to 96-well plates and using a platereader. The viable cell value was calculated as a fraction of the value obtained from cells incubated with fresh medium only.

5.2.8. Cyclooxygenase (COX) enzymatic assay

Compounds were tested for their ability to inhibit the two COX isoforms by using COX inhibitor screening assay kit supplied by the Cayman Chemical Company (Ann Arbor, MI, USA) according to the protocols provided by the manufacturer. This kit includes ovine COX-1 and human recombinant COX-2 enzymes, and it measures percent inhibition of prostaglandin production by the various compounds for the two COX isoforms.

5.3. In vivo anti-inflammatory activity

5.3.1. Animal experiments

Male Wistar strain albino rats weighing 180–200 g were used throughout the assay. They were acquired from a closed random bred colony at the Faculty of Veterinary Medicine, University of Alexandria, Egypt. Rats were given ad libitum access to food and water and housed in groups of four in isolated cages under standard conditions of light and temperature. The animals were acclimatized for 2 weeks prior to experiments. The investigation conformed to the guide for the Care and Use of Laboratory Animals published by US National Institute of Health (NIH Publication No. 83-23, revised 1996). The Local Ethics Committee approved this study.

5.3.2. Formalin-induced paw edema bioassay

This acute inflammatory model was performed as previously described.[35] The rats were randomly divided into groups of five with one group as a control. The other groups received the standard drug celecoxib or the test compounds (at a dose of 20 mg/kg body weight po). A solution of formalin (2%, 0.1 mL) was injected into the subplanter region of the left hind paw under light ether anesthesia 1 h

after oral administration (po) of the test compound (at a dose level of 20 mg/kg body weight). The paw volume (mL) was measured by means of water plethysmometer and re-measured again 1, 2, 3, and 4 h after administration of formalin. The edema was expressed as an increase in the volume of paw, and the percentage of edema inhibition for each rat and each group was obtained as follows:

$$\% \text{ Inhibition} = ((V_t - V_o)_{\text{control}} - (V_t - V_o)_{\text{tested compound}})/(V_t - V_o)_{\text{control}} \times 100$$

where V_t is the volume of edema at specific time interval, V_o is the volume of edema at zero time interval.

5.3.3. Formalin-induced paw edema bioassay

This sub-acute inflammatory model was performed as previously described.[35] Rats in the first experiment were given the same test compounds at a dose level of 20 mg/kg body weight daily for 7 consecutive days. A solution of formalin (2%, 0.1 mL) was injected into the subplanter region of the left hind paw under light ether anesthesia 1 h after oral administration (po) of the test compound. A second injection of formalin (2%, 0.1 mL) was given on the third day. The changes in the volume of paw were measured plethysmographically at the first and eighth days.

5.3.4. Turpentine oil-induced granuloma pouch bioassay

This sub-acute inflammatory model was performed as previously described.[35b,36] A subcutaneous dorsal granuloma pouch was made in ether-anesthetized rats by injecting 2 mL of air, followed by injection of 0.5 mL of turpentine oil into it. All of the test compounds were administered orally (at a dose level of 20 mg/kg body weight) one h prior to turpentine oil injection and continued for seven consecutive days. On the eighth day, the paw was opened under anesthesia and the exudates were taken out with a syringe. The volume (mL) of the exudates was measured and the percentage inhibition of inflammation relative to the control was determined as follows:

$$\% \text{ Inhibition} = (V_{\text{control}} - V_{\text{treated}})/V_{\text{control}} \times 100$$

5.3.5. Ulcerogenic activity

This assay was performed as previously described.[35b,37] The rats were divided into groups of five animals and were fasted for 12 h prior to the administration of the test compounds. Water was given ad libitum. Control group received 1% gum acacia orally. Other groups received indomethacin, celecoxib or the test compounds orally in two equal doses at 0 and 12 h for three successive days at a dose of 300 mg/kg per day. Animals were sacrificed by diethyl ether 6 h after the last dose and their stomachs were removed. An opening at the greater curvature was made and the stomach was cleaned by washing with cold saline and inspected with a 3× magnifying lens for any evidence of hyperemia, hemorrhage, definite hemorrhagic erosion or ulcer.

5.3.6. Acute toxicity

This assay was performed as previously described.[35b] Four groups of rats, each consisting of five animals, were used in this test. The animals were fasted for 24 h prior to administration of the test compounds. The compounds were given in graded doses of 0.1–3.0 g/kg body weight, po. Their acute lethal doses (ALD_{50}) and the mortalities were recorded at each dose level after 24 h.

5.3.7. Determination of effective dose 50 (ED_{50})

The selected compounds were further tested at 5, 10, 20, 40, and 50 mg/kg body weight and the ED_{50} was determined by measuring the inhibition of edema volume 3 h after formalin injection.

5.3.8. Statistical analysis

Data are presented as means ± standard error of the mean (SEM). The concentration-dependent effects of various drugs in vitro were evaluated statistically by the randomized block design analysis of variance (ANOVA). Data obtained in animal studies were subjected to ANOVA, followed by Student–Newman–Keuls Multiple Comparison Test. The difference in results was considered significant when $P < 0.05$.

6. Modeling studies

Computer-assisted simulated docking experiments were carried out under an MMFF94X force field in COX-2 structure (PDB ID: 1CX2) using Chemical Computing Group's Molecular Operating Environment (MOE-dock 2008) software, Montréal, Canada.

Supplementary data

Instrumental data of some compounds is available free of charge via the Internet at http://pubs.acs.org.

Acknowledgments

The authors gratefully acknowledge financial support provided by grants from the Natural Sciences and Engineering Research Council of Canada, the Jack Brown and Family Alzheimer's Disease Research Foundation, and the I.K. Barber School of Arts and Sciences, UBC Okanagan. The authors also thank Dr. Patrick Shipman for valuable discussions and instrumental help.

References and notes

1. (a) Rzepecki, P.; Wehner, M.; Molt, O.; Zadmard, R.; Harms, K.; Schrader, T. *Synthesis* **2003**, *12*, 1815; (b) Rzepecki, P.; Nagel-Steger, L.; Feuerstein, S.; Linne, U.; Molt, O.; Zadmard, R.; Aschermann, K.; Wehner, M.; Schrader, T.; Riesner, D. *J. Biol. Chem.* **2004**, *279*, 47497. and references therein.
2. (a) Fraley, M. E.; Hoffman, W. F.; Rubino, R. S.; Hungate, R. W.; Tebbon, A. J.; Rutledge, R. Z.; McFall, R. C.; Huckle, W. R.; Kendall, R. L.; Coll, K. E.; Thomas, K. A. *Bioorg. Med. Chem. Lett.* **2002**, *12*, 2767; (b) Huang, Y.; Hu, X.; Shen, D.; Chen, Y.; Xu, P. *Mol. Divers.* **2007**, *11*, 73; (c) Wilson, W. L.; Bottiglieri, N. G. *Cancer Chemother. Rep., Part 1* **1962**, 137.
3. Kaymakcioglu, B. K.; Rollas, S.; Korcegez, E.; Aricioglu, F. *Eur. J. Pharm. Sci.* **2005**, *26*, 97.
4. (a) Bekhit, A. A.; Ashour, H. M. A.; Guemei, A. A. *Arch. Pharm. Chem. Life Sci.* **2005**, *338*, 167; (b) Tanitame, A.; Oyamada, Y.; Ofuji, K.; Fujimoto, M.; Iwai, N.; Hiyama, Y.; Suziki, K.; Ito, H.; Terauchi, H.; Kawasaki, M.; Nagai, K.; Wachi, M.; Yamagishi, J. *J. Med. Chem.* **2004**, *47*, 3693; (c) Tanitame, A.; Oyamada, Y.; Ofuji, K.; Kyoya, Y.; Suziki, K.; Ito, H.; Kawasaki, M.; Nagai, K.; Wachi, M.; Yamagishi, J.-i. *Bioorg. Med. Chem. Lett.* **2004**, *14*, 2857; (d) Langer, P.; Wuckelt, J.; Doring, M.; Schreiner, P. R.; Gorls, H. *Eur. J. Org. Chem.* **2001**, 2257.
5. (a) Oruc, E. E.; Kocyigit-Kaymakcioglu, B.; Oral, B.; Altunbas-Toklu, H. Z.; Kabasakal, L.; Rollas, S. *Arch. Pharm. Chem. Life Sci.* **2006**, *339*, 267; (b) Tabarelli, Z.; Rubin, M. A.; Berlese, P. D.; Sauzem, T. P.; Misio, M. V.; Teixeira, A. P.; Sinhorin, A. P.; Martins, M. A. P.; Zanatta, N.; Bonacorso, H. G.; Mello, C. F. *Braz. J. Med. Biol. Res.* **2004**, *37*, 1531.
6. Larsen, J. S.; Zahran, M. A.; Pedersen, E. B.; Nielson, C. *Monatsh. Chem.* **1999**, *130*, 1167.
7. Kepe, V.; Pozgan, F.; Golobic, A.; Polanc, S.; Kocevar, M. *J. Chem. Soc., Perkin Trans. 1* **1998**, 2813. and references therein.
8. Ho, Y. W.; Wang, I. J. *Dyes Pigm.* **1995**, *29*, 295.
9. (a) Wang, T.; Lamb, M. L.; Scott, D. A.; Wang, H.; Block, M. H.; Lyne, P. D.; Lee, J. W.; Davies, A. M.; Zhang, H.-J.; Zhu, Y.; Gu, F.; Han, Y.; Wang, B.; Mohr, P. J.; Kaus, R. J.; Josey, J. A.; Hoffmann, E.; Thress, K.; Maclntyre, T.; Wang, H.; Omer, C. A.; Yu, D. *J. Med. Chem.* **2008**, *51*, 4672; (b) Mukaiyama, H.; Nishimura, T.; Kobayashi, S.; Komatsu, Y.; Kikuchi, S.; Ozawa, T.; Kamada, N.; Ohnota, H. *Bioorg. Med. Chem.* **2008**, *16*, 909.
10. (a) Zang, P.; Pennel, M.; Wright, J.; Chen, W.; Leleti, M.; Li, Y.; Li, L.; Xu, Y., PCT Int. Appl. WO 2007002293 Chemocentryx, USA.; (b) Cheng, C. C.; Robins, R. K. *J. Org. Chem.* **1956**, *21*, 1240.
11. Saggar, S.; Tucker, T.; Tynebor, R.; Su, D.; Anthony, N.; US Patent Appl. US 20070214422007.
12. (a) Anderson, J.; Cottam, H.; Larson, S. *J. Heterocycl. Chem.* **1990**, *27*, 439; (b) Avila, J. L.; Polegre, M. A.; Robins, R. K. *Comp. Biochem. Physiol. C: Pharmacol. Toxicol. Endrocrinol.* **1986**, *83*, 291; (c) Li, J.; Zhao, Y. F.; Zhao, X. L.; Yuan, X. Y.; Gong, P. *Arch. Pharm. Chem. Life Sci.* **2006**, *339*, 593; (d) Manetti, F.; Santucci, A.; Locatelli, G. A.; Maga, G.; Spreafico, A.; Serchi, T.; Orlandini, M.; Bernardini, G.;

Caradonna, N. P.; Spallarossa, A.; Brullo, C.; Schenone, S.; Bruno, O.; Ranise, A.; Bondavalli, F.; Hoffmann, O.; Bologna, M.; Angelucci, A.; Botta, M. *J. Med. Chem.* **2007**, *50*, 5579.
13. Feurer, A.; Luithle, J.; Wirtz, S.; Koenig, G.; Stasch, J.; Stahl, E.; Schreiber, R.; Wunder, F.; Lang, D. PCT Int. Appl. WO 2004009589, Bayer Healthcare AG, Germany.
14. Schmidt, P.; Druey, J. *Helv. Chim. Acta* **1956**, *39*, 986.
15. Weitzel, K. W.; Wickman, J. M.; Augustin, S. G.; Strom, J. G. *Clin. Ther.* **2000**, *22*, 1254.
16. Revesz, L.; Blum, E.; Di Padova, F. E.; Buhl, T.; Feifel, R.; Gram, H.; Hiestand, P.; Manning, U.; Neumann, U.; Rucklin, G. *Bioorg. Med. Chem. Lett.* **2006**, *16*, 262.
17. (a) Das, J.; Moquin, R. V.; Pitt, S.; Zhang, R.; Shen, D. R.; Mclntyre, K. W.; Gillooly, K.; Doweyko, A. M.; Sack, J. S.; Zhang, H.; Kiefer, S. E.; Kish, K.; McKinnon, M.; Barrish, J. C.; Dodd, J. H.; Schieven, G. L.; Leftheris, K. *Bioorg. Med. Chem. Lett.* **2008**, *18*, 2652; (b) Liu, C.; Lin, J.; Pitt, S.; Zhang, R. F.; Sack, J. S.; Kiefer, S. E.; Kish, K.; Doweyko, A. M.; Zhang, H.; Marathe, P. H.; Trzaskos, J.; Mckinnon, M.; Dodd, J. H.; Barrish, J. C.; Schieven, G. L.; Leftheris, K. *Bioorg. Med. Chem. Lett.* **2008**, *18*, 1874.
18. Frampton, J. E.; Keating, G. M. *Drugs* **2007**, *67*, 2433.
19. Menozzi, G.; Merello, L.; Fossa, P.; Mosti, L.; Piana, A.; Mattioli, F. *Farmaco* **2003**, *58*, 795.
20. (a) El-Gaby, M. S. A.; Atalla, A. A.; Gaber, A. M.; Abd Al-Wahab, K. A. *Farmaco* **2000**, *55*, 596; (b) Gilligan, P. J.; Baldauf, C.; Cocuzza, A.; Chidester, D.; Zaczek, R.; Fitzgerald, L. W.; McElroy, J.; Smith, M. A.; Shen, H.-S. L.; Saye, J. A.; Christ, D.; Trainor, G.; Robertson, D. W.; Hartig, P. *Bioorg. Med. Chem.* **2000**, *8*, 181; (c) He, L.; Gilligan, P. J.; Zaczek, R.; Fitzgerald, L. W.; McElroy, J.; Shen, H.-S. L.; Saye, J. A.; Kalin, N. H.; Shelton, S.; Christ, D.; Trainor, G.; Hartig, P. *J. Med. Chem.* **2000**, *43*, 449.
21. Gaber, H. *Org. Prep. Proced. Int.* **2008**, *40*, 365.
22. Robins, R. K. *J. Am. Chem. Soc.* **1956**, *78*, 784.
23. Quiroga, J.; Portilla, J.; Abonia, R.; Insuasty, B.; Nogueras, M.; Cobo, J. *Tetrahedron Lett.* **2008**, *49*, 6254.
24. Hildick, B.; Shaw, G. *J. Chem. Soc., Perkin Trans. 1* **1971**, *9*, 1610.
25. Nofal, Z.; Fahmy, H.; Kamel, M.; Sarhan, A.; Soliman, G. *Egypt. J. Pharm. Sci.* **2003**, *44*, 155.
26. Gavrilenko, B.; Kapitan, A. *Zh. Org. Khim.* **1984**, *20*, 860.
27. (a) Lindauer, D.; Beckert, R.; Doering, M.; Fehling, P.; Goerls, H. *J. Prakt. Chem./Chem-Ztg* **1995**, *337*, 143; (b) Bonauer, C.; Koenig, B. *Synthesis* **2005**, *14*, 2367.
28. (a) Klegeris, A.; Walker, D. G.; McGeer, P. L. *Neuropharmacology* **1999**, *38*, 1017; (b) Klegeris, A.; Maguire, J.; McGeer, P. L. *J. Neuroimmunol.* **2004**, *152*, 73.
29. Gierse, J. K.; Koboldt, C. M. *Curr. Prot. Pharmacol.* **1998**, 3.1.1.
30. Foucaud, L.; Bennasroune, A.; Klestadt, D.; Laval-Gilly, P.; Falla, J. *Toxicol. In Vitro* **2006**, *20*, 101.
31. Kurumbail, R. G.; Stevens, A. M.; Gierse, J. K.; McDonald, J. J.; Stegeman, R. A.; Pak, J. Y.; Gildehaus, D.; Iyashiro, J. M.; Penning, T. D.; Seibert, K.; Isakson, P. C.; Stallings, W. C. *Nature* **1996**, *384*, 644.
32. Molecular Operating Environment (MOE) 2008.10, Chemical Computing Group Inc., 1010 Sherbrooke Street West, Suite 910, Montréal, H3A 2R7, Canada, <http://www.chemcomp.com/>.
33. Decker, T.; Lohmann-Matthes, M. L. *J. Immunol. Methods* **1988**, *115*, 61.
34. (a) Mosmann, T. *J. Immunol. Methods* **1983**, *65*, 55; (b) Hansen, M. B.; Nielsen, S. E.; Berg, K. *J. Immunol. Methods* **1989**, *119*, 203.
35. (a) Hosseinzadeh, H.; Younesi, H. M. *BMC Pharmacol.* **2002**, *2*, 7; (b) Rostom, S. A. F.; El-Ashmawy, I. M.; Abd El Razik, H. A.; Badr, M. H.; Ashour, H. M. A. *Bioorg. Med. Chem.* **2009**, *17*, 882.
36. Robert, A.; Nezamis, J. E. *Acta Endocr.* **1957**, *25*, 105.
37. Daidone, G.; Maggio, B.; Raffa, D.; Plescia, S.; Bajardi, M. L.; Caruso, A.; Cutuli, V. M. C.; Amico-Roxas, M. *Eur. J. Med. Chem.* **1994**, *29*, 707.